Conformational Analysis of the Xylose-Containing *N*-Glycan of Pineapple Stem Bromelain as Part of the Intact Glycoprotein†

Jos P. M. Lommerse,‡ Loes M. J. Kroon-Batenburg,§ Johannis P. Kamerling,‡ and Johannes F. G. Vliegenthart*,‡

Department of Bio-Organic Chemistry and Department of Crystal and Structural Chemistry, Bijvoet Center, Utrecht University, P.O. Box 80.075, NL-3508 TB Utrecht, The Netherlands

Received December 14, 1994; Revised Manuscript Received April 7, 1995⊗

ABSTRACT: The conformational behavior of the *N*-glycan Manα1−6(Xylβ1−2)Manβ1−4GlcNAcβ1−4(Fucα1−3)GlcNAcβ of stem bromelain as part of the intact glycoprotein was investigated and compared with that of the same *N*-glycan as part of a bromelain-derived glycopeptide. Proton chemical shifts of the glycoprotein *N*-glycan were determined by 2D HOHAHA and 2D NOESY measurements, making use of the glycopeptide ^{1}H NMR data. During each 2D NMR experiment about 4% of the glycoprotein denatured. Experimental data concerning interproton distances of the intact glycoprotein *N*-glycan were obtained by NOESY ^{1}H NMR spectroscopy. Several theoretical models for the *N*-glycan, obtained by molecular dynamics simulations of the glycopeptide, were investigated. Comparison of experimental and theoretical NOESY cross peak intensities was performed with the program CROSREL. In comparison with the glycopeptide, the distribution of populations between two main conformations of the Fucα1−3GlcNAc linkage was altered. In addition, the $\omega = 60°$ (*gt*) rotamer of the Manα1−6Man linkage seems to be present for a significant period of time, whereas in the glycopeptide the $\omega = -60°$ (*gg*) conformation exists exclusively. Except for the Xylβ1−2Man linkage, the mobilities around the glycosidic linkages in the glycoprotein were reduced compared with those in the glycopeptide, especially concerning the Fucα1−3GlcNAc and Manα1−6Man linkages. These findings might be the result of an interaction of the polypeptide chain with the Fucα/Manα side of the *N*-glycan. A qualitative analysis of the NMR spectra showed a larger degree of mobility in the denatured glycoprotein *N*-glycan than in the intact glycoprotein.

In order to understand the mechanism of biological function of oligosaccharide chains as part of glycoproteins, the study of the conformational space explored by these glycans is of essential importance. Several conformational analyses have already been performed on free oligosaccharides or glycopeptides, but only a few have been performed on glycans as part of glycoproteins, mainly by using X-ray crystallography (Shaanan et al., 1991; Vargese & Colman, 1991). Because most glycans are exposed on the surface of the glycoprotein, one should be reluctant to extrapolate X-ray data directly to conformations in the biological, aqueous environment.

The most powerful approach to obtain structural information for biomolecules in solution relies on nuclear Overhauser enhancement (NOE) in NMR experiments. However, there are several complications when glycoprotein glycans are analyzed by NMR. Often several structurally different, but closely related carbohydrate chains are attached to the side chain of one or more amino acid residues in the polypeptide backbone. Due to this microheterogeneity, rarely is only one glycoform present, but rather it is usually a collection of glycoforms. This feature complicates the analysis enormously, enlarging the already existing severe overlap in the ^{1}H NMR spectra, as most carbohydrate signals are found in a small spectral region.

In this study, pineapple stem bromelain was chosen for the analysis of conformation and mobility of an *N*-glycan in its natural environment, because this glycoprotein has only one glycosylation site and no microheterogeneity is present. Moreover, it is possible to study the influence of a folded polypeptide chain on the *N*-glycan, because conformational data for a glycotetrapeptide (Figure 1) derived from this glycoprotein are available (Bouwstra et al., 1990; Lommerse et al., 1995).

Pineapple stem bromelain (EC 3.4.22.4) is a member of the cysteine proteinase family. The primary structure of the *N*-glycan was reported by Ishihara et al. (1979), and ^{1}H NMR data of the *N*-glycan were established by Van Kuik et al. (1986). The amino acid sequence of the polypeptide chain has been determined by Ritonja et al. (1989). Structurally comparable cysteine proteinases, such as papain and actinidin, have been analyzed by X-ray diffraction (Baker, 1980; Kamphuis et al., 1984). A tertiary structure of bromelain has been proposed, as calculated by the alignment of its amino acid sequence to the sequences of papain and actinidin (Kamphuis et al., 1985; Topham et al., 1990). However, no information concerning the conformation of the *N*-glycan in the intact glycoprotein is available.

MATERIALS AND METHODS

Preparation of Pineapple Stem Bromelain. Pineapple stem bromelain (EC 3.4.22.4), purchased from Boehringer Mannheim, Germany, was purified at 4 °C, essentially as described (Rowan et al., 1988), using CM-Sepharose instead of mono

† This project was supported by the Netherlands Foundation for Chemical Research (SON), with financial aid from the Netherlands Organization for Scientific Research (NWO).

* Author to whom correspondence should be addressed (Fax +31-30-540980).

‡ Department of Bio-Organic Chemistry.

§ Department of Crystal and Structural Chemistry.

⊗ Abstract published in *Advance ACS Abstracts,* June 1, 1995.

0006-2960/95/0434-8196$09.00/0

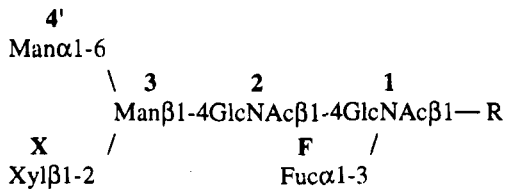

FIGURE 1: Primary structure of the pineapple stem bromelain *N*-glycan. For the glycoprotein, R represents a polypeptide chain. For the glycopeptide, R represents [NH_2-]-Asn-Glu-Ser-Ser-COOH.

S. The proteinase activity of bromelain samples was determined by using azocasein as a substrate (Rowan et al., 1988). Circular dichroism (CD) measurements were performed at 37 °C in 0.2 mm light pathway cells in a Jasco-600 spectropolarimeter, interfaced to a Laser 386 computer, while flushing the cuvette chamber with nitrogen gas. After subtraction of the control protein-free sample, the CD spectra were fitted to four reference spectra, using a nonlinear least-squares fit procedure, in order to determine the amounts of α-helix, β-strand, β-turn, and random coil. The reference spectra for the α-helix, β-strand, and random coil were taken from CD spectra of $(Lys)_n$ (Greenfield & Fasman, 1969), and that for β-turn was the average of 15 proteins (Chang et al., 1978).

^1H NMR Measurements. Homonuclear 2D ^1H NMR spectra of bromelain were recorded on a Bruker AMX-600 spectrometer and spectra of the bromelain-derived glycopeptide (Bouwstra et al., 1990; Lommerse et al., 1995) were recorded on a Bruker AMX-500 spectrometer, operating at 600 and 500 MHz, respectively (Department of NMR Spectroscopy, Bijvoet Center, Utrecht University, The Netherlands) at a probe temperature of 315 K. The NOESY spectra of the glycopeptide, measured at 300 K, were obtained previously (Lommerse et al., 1995). Chemical shifts (δ) are expressed in ppm downfield from internal sodium 4,4-dimethyl-4-silapentane-1-sulfonate, but were actually measured by reference to internal acetone (δ 2.225; Vliegenthart et al., 1983). Suppression of the $^1HO^2H$ signal was performed by presaturation during the relaxation delay for 1 s. Each 2D spectrum consisted of a 512 × 4K data matrix.

Four 2D NOESY (Macura & Ernst, 1983) spectra of bromelain were recorded in succession with mixing times of 25, 50, 80, and 115 ms, taking a total of 40 h measuring time. Subsequently, two 2D HOHAHA (Bax & Davis, 1985) spectra were measured for the sample, using 40 and 80 ms MLEV-17 mixing sequences, respectively, at a field strength of 9.4 kHz (90° pulse width of 26.7 μs). The spectral width was 6667 Hz in each dimension. A 2D HOHAHA experiment on the glycopeptide was performed using a 80 ms MLEV-17 mixing sequence at a field strength of 9.6 kHz (90° pulse width of 26.1 μs). The spectral width was 4030 Hz in each dimension.

The data matrices obtained (512 × 4K) were processed on a Silicon Graphics 3D/35 computer, using the TRITON software (R. Kaptein and R. Boelens, Department of NMR Spectroscopy, Utrecht University). The time domain data were weighted with a $\pi/3$ shifted sine-bell in both dimensions. After zero-filling and Fourier transformation, 1K × 4K spectra were obtained.

The 2D NOESY spectra were baseline corrected by a fit to a straight line in ω_1. The cross peaks were integrated in a rectangular area around the peak maximum and were corrected for the local baseline errors by subtracting an average of the integrated equal rectangular areas around the location of the cross peak. Peak integration in the NOESY spectra of the glycoprotein turned out to be less accurate than in the NOESY spectra of the glycopeptide due to larger baseline errors and line broadening. In order to estimate the standard deviation of integration, five independent integrations were carried out for each cross peak using different sizes of the integrated rectangular areas around the cross peak maximum, as well as different spots for subtraction of the local baseline area. By using a least-squares fitting procedure (Press et al., 1986) to a parabolic function, an approximated standard deviation was calculated for effective rotation correlation times ($\tau_{eff,k}$, see Appendix).

Oligosaccharide Mobility. The computer program CROSREL (Leeflang & Kroon-Batenburg, 1992) was used in order to calculate the NOEs of a given three-dimensional model of the *N*-glycan, as described previously for the bromelain glycopeptide (Lommerse et al., 1995).

The calculation procedure, which applies effective rotation correlation times for each monosaccharide residue, is referred to as method III (Lommerse et al., 1995). The effective rotation correlation time of monosaccharide residue k ($\tau_{eff,k}$) is obtained by fitting NOE intensities to the experiment using the spectral density function $J_n(\omega)$:

$$J_n(\omega) = \langle r_{ij}^{-3} \rangle^2 \frac{\tau_{eff,k}}{1 + (n\omega\tau_{eff,k})^2} \quad (1)$$

in which r_{ij} is the average distance between protons i and j and ω is their Larmor frequency. The overall rotation correlation time (τ_o), the slow internal rotation correlation time ($\tau_{s,k}$), and the fast internal motions, which can be described by the generalized order parameter S_f^2, are included in $\tau_{eff,k}$ [see Lommerse et al. (1995)].

A simplified model, which assumes that the oligosaccharide chain tumbles isotropically, is described by method I (Lommerse et al., 1995). In this model, all effective rotation correlation times are equal throughout the molecule; thus, the molecular motions are described by one overall rotation correlation time τ_o:

$$J_n(\omega) = \langle r_{ij}^{-3} \rangle^2 \frac{\tau_o}{1 + (n\omega\tau_o)^2} \quad (2)$$

Note that this model considers average distances from MD trajectories. In the case of the bromelain *N*-glycan, which is attached to the polypeptide backbone, it is preferable to denote its overall rotation correlation time by *mean* rotation correlation time, because the overall motion is associated with the whole molecule (glycoprotein), whereas a part of the molecule (the *N*-glycan) will experience a different average motion.

Characteristic times of glycosidic conformational transitions can be calculated from the effective rotation correlation times of the monosaccharide residues involved (Lommerse et al., 1995). The motion of a certain monosaccharide residue is regarded as the sum of the motions of the flexible glycosidic linkages and the motion of a less mobile, preceding residue (Figure 2). If interactions are only present between two connected monosaccharide residues, then the residues more remote from the center of mass will have

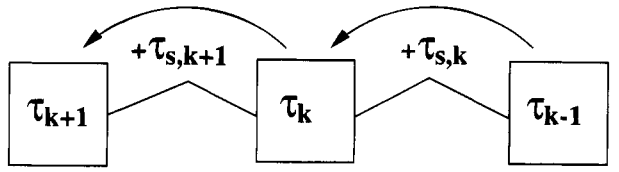

FIGURE 2: Addition of motions within an oligosaccharide chain.

Table 1: Calculated Amounts of Secondary Structure and Relative Proteinase Activity of Pineapple Stem Bromelain, with and without Irreversible Inhibitor E-64 and before and after 44 h of Incubation at 37 °C

		secondary structure (%)				relative
sample	inhibitor	α-helix	β-strand	β-turn	random coil	proteinase activity (%)
freshly prepared sample	without E-64	27	20	12	41	100
	with E-64	28	19	13	40	0
after 44 h of incubation at 37 °C	without E-64	22	22	10	46	72
	with E-64	26	19	13	41	0

smaller rotation correlation times. This can be expressed by the reciprocal sum of the rotation correlation times of the residue $(k - 1)$, being closest to the center of mass, and the rotation correlation time of the glycosidic linkage k in between the residues:

$$\tau_k^{-1} = \tau_{k-1}^{-1} + \tau_{s,k}^{-1} \quad (3)$$

and for the next residue $(k + 1)$ in the chain:

$$\tau_{k+1}^{-1} = \tau_k^{-1} + \tau_{s,k+1}^{-1} = \tau_{k-1}^{-1} + \tau_{s,k}^{-1} + \tau_{s,k+1}^{-1} \quad (4)$$

RESULTS AND DISCUSSION

Preparation of Bromelain. Purification of the bromelain preparation by cation-exchange chromatography yielded two major fractions, representing the two forms I and II of the glycoprotein (Rowan et al., 1988). Both forms have almost identical proteinase activity toward azocasein. They do not interchange, because they appear as single peaks after rechromatography of each form under the same conditions. Samples for CD and NMR measurements were prepared from glycoprotein form I.

In order to obtain information concerning the stability of the bromelain preparation, CD measurements were carried out and the results are listed in Table 1. The calculated relative amounts of the various secondary structures of a freshly prepared bromelain sample without inhibitor E-64 [*N*-[*N*-(L-3-*trans*-carboxyoxiranyl-2-carbonyl-L-leucyl)]agmatine] were 27% α-helix, 20% β-strand, 12% β-turn, and 41% random coil. These values are similar to those reported for papain (Yang et al., 1986), having on average up to 27% α-helix, 7% β-strand, 18% β-turn, and 48% random coil. These amounts of secondary structure are in agreement with a model of the three-dimensional structure of the bromelain polypeptide chain, as calculated by the alignment of the bromelain amino acid sequence with those of the cysteine proteinases papain and actinidin studied by X-ray diffraction (Kamphuis et al., 1985; Topham et al., 1989). The sample of bromelain inactivated by the irreversible inhibitor E-64 resulted in an almost identical CD spectrum, indicating that only minor overall changes have been induced by E-64 (see Table 1). After incubation for 44 h at 37 °C, the average secondary structure of bromelain without E-64 changed significantly, resulting in a decrease in the relative amount of α-helix. The changes, most probably caused by autodigestion, are also evident from the decrease in proteinase activity to 72% of its original value. In contrast, the CD spectrum of bromelain inactivated by E-64 barely changed after 44 h of incubation; only a slight decrease in the α-helix content can be observed. Because bromelain inactivated by E-64 is relatively stable at elevated temperatures, such a preparation was used for the NMR measurements.

^{1}H NMR Measurements: Partial Denaturation of the Glycoprotein. In order to obtain good quality spectra of the glycoprotein, the ^{1}H NMR measurements were performed at 315 K. At lower temperatures, the proton signals suffered from fast T_2 relaxation, leading to line broadening.

In the NOESY spectra (Figure 3; 115 ms), the cross peaks between the various *N*-glycan protons are clearly resolved from the cross peaks between the polypeptide chain protons. Usually, as in this case, only a few NOE contacts between amino acid residues are found in the monosaccharide spectral region δ 5.2−3.2 (Wüthrich, 1986). Inspection of the NOESY spectra showed that the strong NOE contacts are accompanied by satellite cross peaks. The intensity of the satellite cross peaks increased in the NOESY spectra with the same mixing time (115 ms), but measured 30 and 50 h later, respectively. This observation suggests some denaturation of the E-64-inactivated bromelain, giving rise to the satellite cross peaks.

In contrast to the NOESY spectra, the HOHAHA spectra (Figure 4; 80 ms) yielded strong cross peaks for the denatured glycoprotein *N*-glycan, whereas those of the intact glycoprotein were relatively weak. The carbohydrate-derived NOESY and HOHAHA cross peaks originating from the intact glycoprotein are rather broad in comparison with those of the denatured form, which is nicely illustrated at the Man-**3** H-1 ω_1 track in the NOESY spectrum of the intact glycoprotein compared to that of the denatured glycoprotein (Figure 3).

It is likely that the differences in intensity and line shape of the cross peaks between the intact and denatured glycoproteins, observed in the HOHAHA and NOESY spectra, are caused by a difference in the mobility of the oligosaccharide chain. In the case of denaturation, the mobility of the oligosaccharide chain is probably increased, as compared to the situation in which the oligosaccharide chain is near the folded polypeptide chain of the intact glycoprotein. The *N*-glycan of the intact glycoprotein is less mobile and will experience a longer rotation correlation time, resulting in fast T_2 relaxation times and broader peaks. Other consequences of the longer rotation correlation time are a faster NOE build-up rate and a larger decay of magnetization during the spin−lock time in the HOHAHA experiment (Bax & Davis, 1985), as compared to the denatured glycoprotein. The relatively intense cross peaks within the spin systems of the Man-**4′** and Xyl residues in the intact glycoprotein in the HOHAHA spectrum are explained by their larger mobility compared to the other residues in the *N*-glycan, as will be shown later. Only weak (satellite) cross peaks are found in the NOESY

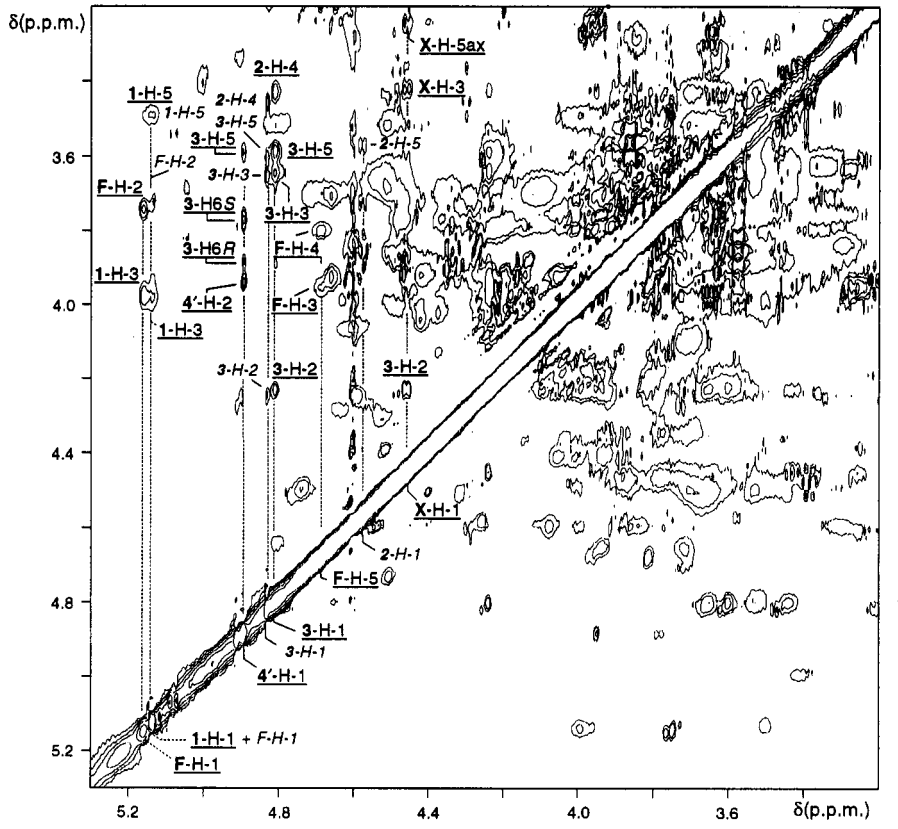

FIGURE 3: 2D $^1H-^1H$ NOESY spectrum, with mixing time 115 ms, of bromelain recorded in ^2H_2O measured at a probe temperature of 315 K. Abbreviations used: **1**, β-D-GlcNAc-1; **2**, β-D-GlcNAc-2; **3**, β-D-Man-3; **4′**, α-D-Man-4′; **F**, α-L-Fuc; **X**, β-D-Xyl. Underlined proton signals are from the intact glycoprotein, whereas the italic designations are those of the denatured glycoprotein.

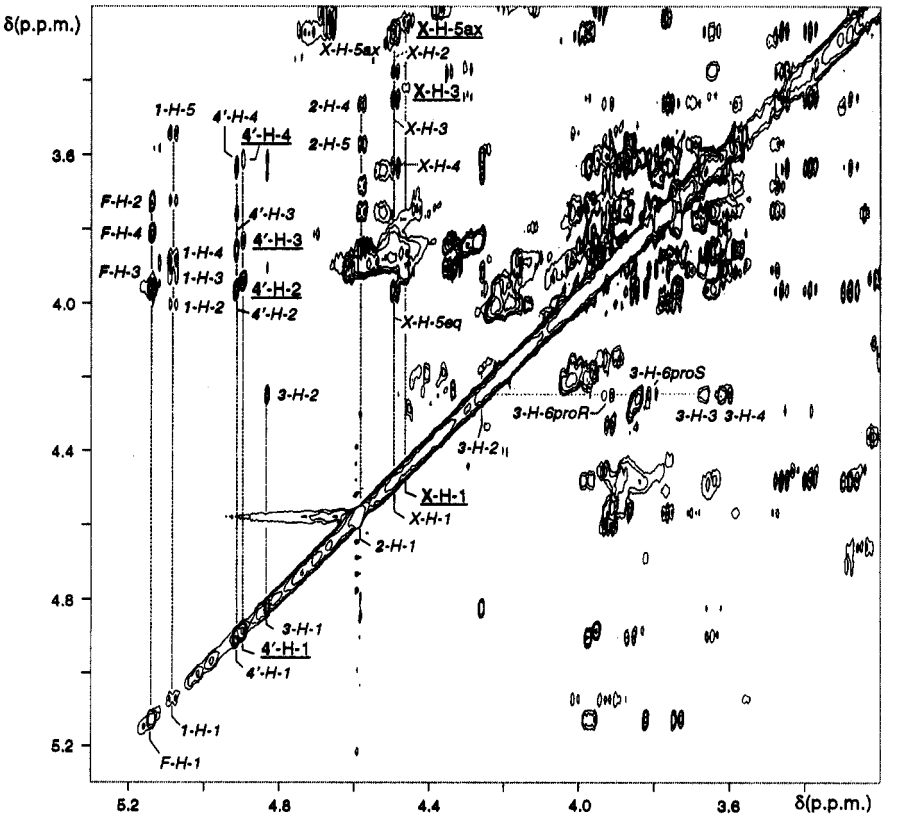

FIGURE 4: 2D $^1H-^1H$ HOHAHA spectrum, with mixing time 80 ms, of bromelain recorded in ^2H_2O measured at a probe temperature of 315 K. Abbreviations and designations used are the same as for Figure 3.

Table 2: ^{1}H NMR Chemical Shift Values (ppm) of the Bromelain *N*-Glycan Protons, as Part of the Intact and Denatured Glycoproteins (315 K) and Those as Part of the Glycopeptide [315 and 300 K, According to Bouwstra et al. (1990)]

		glycopeptide		glycoprotein	
proton		300 K	315 K	315 K (native)	315 K (denatured)
GlcNAc-**1**	H-1	5.121	5.122	5.126	5.081
	H-5	3.575	3.592	3.495	3.552
GlcNAc-**2**	H-1	4.597	4.576	~4.6	4.579
	H-4	3.458	3.466	3.443	3.471
Man-**3**	H-1	4.839	4.828	4.812	4.833
	H-2	4.262	4.257	4.240	4.259
	H-6-*pro-R*	3.892	3.919	3.892	3.922
	H-6-*pro-S*	3.723	3.798	3.786	3.805
Man-**4′**	H-1	4.913	4.910	4.896	4.914
	H-2	3.972	3.970	3.952	3.975
	H-3	3.863	3.858	3.836	3.863
Xyl	H-1	4.470	4.484	4.463	4.490
	H-2	3.376	3.380	3.370	3.388
	H-3	3.452	3.458	3.433	3.462
	$H\text{-}5_{ax}$	3.270	3.274	3.255	3.280
Fuc	H-1	5.136	5.131	5.162	5.138
	H-2	3.721	3.734	3.759	3.738
	H-3	3.981	3.969	3.965	nd[a]
	H-4	3.814	3.818	3.814	3.823
	H-5	4.722	4.687	4.691	4.704
	CH_3	1.285	1.278	1.284	1.282

[a] nd, not detected.

spectra for the small amount of denatured glycoprotein *N*-glycan, because it experiences a slower NOE build-up rate. Almost no NOE cross peaks have arisen from its terminal, and probably most mobile, residues Man-**4′** and Xyl.

The chemical shift values at 315 K of a series of *N*-glycan protons as part of the glycopeptide, part of the intact glycoprotein, and part of the denatured glycoprotein, assigned by comparison with the ^{1}H NMR data for the glycopeptide at 300 K (Bouwstra et al., 1990), are listed in Table 2. Several signals of the glycoprotein *N*-glycan could not be determined due to spectral overlap or due to too low intensities. Most differences between the established proton chemical shifts of the intact glycoprotein *N*-glycan and the glycopeptide at 315 K are within $\Delta\delta$ ±0.030. These observations are similar to those reported for a triantennary oligosaccharide, measured as part of the glycoprotein hen phosvitin (Brockbank & Vogel, 1990) and as part of a glycopeptide (Joziasse et al., 1987). In the intact bromelain most δ values are shifted upfield as compared to the glycopeptide, but near the glycosylation site clear downfield shifts are observed (GlcNAc-**2** H-1, Fuc H-1, and Fuc H-2). In this context, the upfield shift of GlcNAc-**1** H-5 ($\Delta\delta$ −0.097) is remarkable.

Most chemical shift values of the denatured glycoprotein *N*-glycan are close to those of the glycopeptide; only GlcNAc-**1** H-1 and H-5 show large upfield shifts ($\Delta\delta$ −0.04). This observation points to similar environments for the *N*-glycan in the denatured glycoprotein and in the glycopeptide. Differences in chemical shift values between the corresponding *N*-glycan protons of the intact glycoprotein and the denatured glycoprotein possibly reflect interaction of the *N*-glycan with the intact polypeptide chain.

The NOE cross peak intensities of the NOESY build-up series were corrected for the denaturing process as follows. From three NOESY spectra, all with the same mixing time of 115 ms, the rate of denaturation was quantified by integration of cross peak intensities of the *N*-glycan. During each NMR experiment (taking about 10 h), 4% of the total amount of the intact bromelain turned out to be converted into denatured glycoprotein. This denaturing rate was used for correction of the NOESY build-up series by normalizing the cross peak intensities of the intact glycoprotein in the first NOESY experiment (mixing time 25 ms, amount of intact glycoprotein is 100%) and increasing the intensities of the three following experiments (50, 80, and 115 ms) as if 100% intact glycoprotein was still present.

Theoretical Models of the N-Glycan from MD Simulations. The conformational analysis of the bromelain *N*-glycan as part of the intact glycoprotein was performed using the CROSREL program, which allows the comparison of theoretical models with experimental data from the NOESY build-up series. Recently, theoretical models for this glycan as part of the glycotetrapeptide were obtained from molecular dynamics (MD) simulations at 300 K, using the Gromos program package (Lommerse et al., 1995). Three long MD trajectories (A, B, and C, respectively) and ten parts of short MD trajectories (D1−D10), as conformational probes stable for at least 30 ps, were analyzed. The corresponding average dihedral angles of the glycosidic linkages are listed in Table

Table 3: Average Values for the Dihedral Angles of the Glycosidic Linkages[a] of the Long MD Trajectories (A−C) and of the Conformational Probes (D1−10) of a Glycopeptide of Bromelain

		M4′α1−6M3			Xβ1−2M3		M3β1−4G2		G2β1−4G1		Fα1−3G1	
trajectory	*t* (ps)	ϕ	ψ	ω	ϕ	ψ	ϕ	ψ	ϕ	ψ	ϕ	ψ
A	260	117	180	−6	−85	−102	−74	108	−67	125	−102	−111
B	460	104	−177	64	−78	−97	−74	110	−57	128	−145	−141
C	460	117	−179	3	−75	−102	−83	106	−70	126	−125	−126
D1	40	166	177	−52	−62	−93	−61	110	−72	124	−92	−105
D2	70	159	180	−56	−82	−103	−70	114	−70	130	−157	−147
D3	30	156	177	−59	−89	−105	−57	116	−55	132	−141	−140
D4	30	147	176	−49	−88	−108	−59	109	−49	132	−138	−136
D5	50	147	177	−41	−85	−111	−92	84	−64	133	−133	−134
D6	30	76	175	51	−94	−102	−71	99	−76	129	−154	−146
D7	30	83	−161	52	−80	−78	−85	101	−64	134	−143	−134
D8	70	90	−172	62	−69	−89	−97	99	−78	119	−94	−103
D9	35	119	−173	65	−68	−94	−88	103	−75	121	−94	−104
D10	35	142	−142	68	−132	−140	−81	107	−76	122	−90	−99

[a] Abbreviations used: M, Man; X, Xyl; G, GlcNAc; F, Fuc. According to IUPAC definitions (IUPAC−IUB (JBCN), 1983). The dihedral angles of the glycosidic linkage (ϕ,ψ) for monosaccharide A(1→*x*)monosaccharide B are defined as follows: ϕ = ($O5_A$,$C1_A$,Ox_B,Cx_B), ψ = ($C1_A$,Ox_B,Cx_B,$Cx-1_B$). In this study ω is defined by ($O6_B$,$C6_B$,$C5_B$,$O5_B$).

Table 4: Mean (τ_{mean}, Intact Glycoprotein), Overall ($\tau_{overall}$, Glycopeptide), and Individual Effective Rotation Correlation Times (ns) for Each Monosaccharide Residue of the Bromelain *N*-Glycan, Determined for the MD Trajectories A, B, and C, Respectively

N-Glycan as Part of the Intact Glycoprotein

		$\tau_{eff,k}$					
	τ_{mean}	Man-**4′** H1,2	Xyl H1,5_{ax}	Man-**3** H1,2	GlcNAc-**2**[a] H1,5	GlcNAc-**1** H1,5	Fuc H1,2
A	9.7	5.4	4.5	13.0	15.0	17.7	11.6
B	9.4	5.3	4.6	13.5	15.2	17.4	10.1
C	8.9	4.9	4.1	11.7	14.2	18.0	10.1

N-Glycan as Part of the Glycopeptide

		$\tau_{eff,k}$					
	$\tau_{overall}$	Man-**4′** H1,2	Xyl H1,5_{ax}	Man-**3** H1,2	GlcNAc-**2**[a] H1,5	GlcNAc-**1** H1,5	Fuc H1,2
A	0.67	0.50	0.66	0.75	0.85	0.81	0.59
B	0.67	0.51	0.69	0.79	0.79	0.84	0.59
C	0.67	0.51	0.67	0.76	0.84	0.87	0.59

[a] Due to a lack of NOE data, the effective rotation correlation time of GlcNAc-**2** was approximated as intermediate between those of Man-**3** and GlcNAc-**1** and was not included in the calculation of the mean rotation correlation time.

Table 5: R_w Values of the Fits of $^1H-^1H$ Pairs of the Bromelain *N*-Glycan for the Long MD Trajectories A–C Using Calculation Methods I and III (see Text)

(a) R_w Values of the Fits of Five Intraresidual $^1H-^1H$ Pairs (See Table 4)

	glycopeptide[a]		glycoprotein	
trajectory	I	III	I	III
A	0.363	0.117	0.270	0.063
B	0.373	0.115	0.259	0.062
C	0.375	0.112	0.285	0.062

(b) R_w Values of the Fits of Five Interresidual $^1H-^1H$ Pairs (See Table 6)

	glycopeptide[a]		glycoprotein	
trajectory	I	III	I	III
A	1.032	0.639	0.774	0.479
B	0.735	0.481	0.723	0.367
C	1.220	0.874	0.972	0.629

[a] For comparison, the same five intra- and interresidual NOE build-up curves as for the glycoprotein were taken.

3. Average $^1H-^1H$ distance matrices were calculated by $r = \langle r^{-3} \rangle^{-1/3}$.

The MD trajectories of the glycopeptide can provide possible average conformations for the glycoprotein *N*-glycan. However, it is not possible to extract the generalized order parameters S_f^2 from these trajectories to be used for the calculation of NOEs of the glycoprotein *N*-glycan (methods II and IV; Lommerse et al., 1995). First, the internal motions of the oligosaccharide chain in the glycoprotein can be different from those in the glycopeptide, and second, the MD simulations were performed at a temperature (300 K) different from that of the NOESY experiments of the glycoprotein (315 K). Therefore, in this paper calculations have been carried out using methods I and III only. For method I, which is based on eq 2, one mean rotation correlation time is used to describe motions for the whole *N*-glycan. Method III, based on eq 1, applies one effective rotation correlation time for each monosaccharide residue.

The diagonal peak intensities could not be measured reliably in the 2D NOESY spectra. Therefore, Obs-scaling was used in the CROSREL program (Leeflang & Kroon-Batenburg, 1992). All experimental NOE cross peaks were scaled by one overall scaling factor (osf) for each theoretical model. The determination of the osf was performed by fitting one mean rotation correlation time to the experimental data of five available intraresidual NOE intensities, one of each monosaccharide residue of the glycoprotein *N*-glycan (see Table 4). No intraresidual NOE intensities were available for GlcNAc-**2**. An effective local rotation correlation time for each of the five monosaccharide residues was obtained by fitting the NOE intensities of its intraresidual $^1H-^1H$ pair to the experiment, using the calculated osf. A new fit of the intraresidual NOE intensities barely changed the osf (about 1%), indicating that the osf had been determined adequately. The same procedure was also performed for the glycopeptide using six available intraresidual NOEs (see Table 4).

The same intra- and interresidual NOEs that were taken previously for the glycopeptide (Lommerse et al., 1995; without those of GlcNAc-**2** H-1) were chosen to evaluate the quality of the fit of the models using R_w values (Leeflang & Kroon-Batenburg, 1992). The R_w values for both the

Table 6: R_w Values[a] for the Various MD Trajectories of the Individual Interresidual NOEs of the Bromelain *N*-Glycan as Part of the Intact Glycoprotein and as Part of the Glycopeptide, Using Calculation Method III

	bromelain glycoprotein					bromelain glycopeptide				
	Man-**4′**H-1/ Man-**3** H-6-*pro-S*	Man-**4′**H-1/ Man-**3** H-6-*pro-R*	Xyl H-1/ Man-**3** H-2	Man-**3** H-1/ GlcNAc-**2** H-4	Fuc H-1/ GlcNAc-**1** H-3	Man-**4′**H-1/ Man-**3** H-6-*pro-S*	Man-**4′**H-1/ Man-**3** H-6-*pro-R*	Xyl H-1/ Man-**3** H-2	Man-**3** H-1/ GlcNAc-**2** H-4	Fuc H-1/ GlcNAc-**1** H-3
A	+/−0.035	+1.694	−0.365	+0.210	+/−0.399	−0.309	+0.754	+0.342	+0.192	+1.403
B	+/−0.053	+1.569	−0.169	+0.144	+/−0.125	−/+0.253	+0.665	+0.769	+0.127	+0.621
C	−/+0.030	+0.659	−0.269	+0.717	+0.515	−0.319	+1.047	+0.520	+0.647	+1.681
D1	−0.363	+1.517	−0.699	−0.211	+/−0.485	−0.704	+1.163	−0.409	−0.305	+1.578
D2	−0.141	+2.441	−0.122	+0.121	−0.426	−0.545	+2.050	+0.841	−/+0.137	−0.129
D3	−0.078	+2.624	+0.216	−0.373	+0.327	−0.471	+2.206	+1.577	−0.487	+1.048
D4	−0.037	+2.366	+0.252	−0.245	+0.581	−0.378	+1.710	+1.658	−0.312	+1.900
D5	−0.113	+1.964	+0.173	+0.511	+0.984	−0.432	+1.387	+1.498	+0.469	+2.834
D6	+/−0.071	+0.967	+0.178	+0.145	−0.323	−/+0.222	−/+0.368	+1.612	−/+0.129	+0.073
D7	−0.080	+1.806	−0.668	+0.438	+0.298	−0.393	+1.052	−0.336	+0.919	+1.275
D8	+/−0.027	+1.668	−0.615	+1.001	+0.601	−0.343	−/+0.617	−0.209	+1.069	+1.854
D9	+0.151	+2.909	−0.596	+0.829	+/−0.508	−0.326	+2.117	−0.184	+1.089	+1.695
D10	+0.611	+6.684	+0.397	+0.633	+0.318	−0.506	+6.106	+2.121	+0.801	+1.062

[a] −, +, and +/− indicate that the calculated NOE build-up curve is weaker than, larger than, or going through, respectively, the experimental curve.

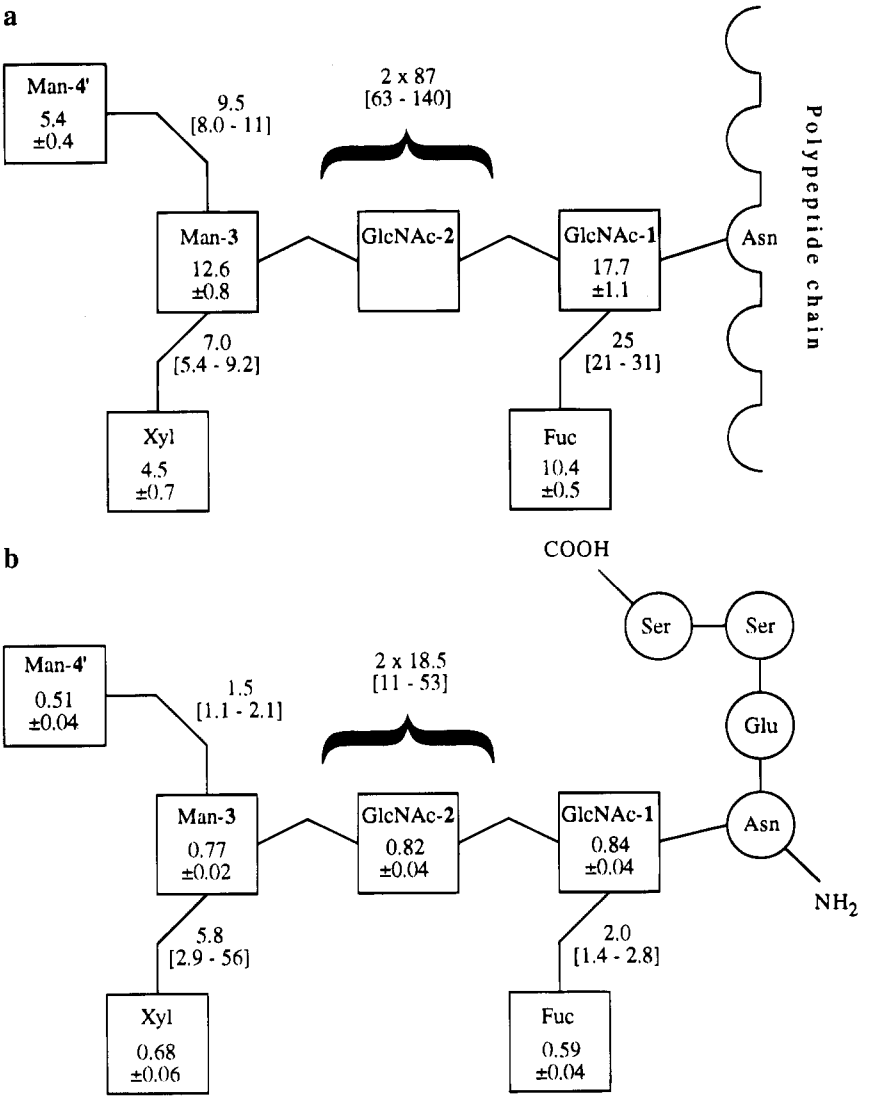

FIGURE 5: Effective rotation correlation times ($\tau_{eff,k}$, ns) of the different monosaccharide residues and slow internal rotation correlation times ($\tau_{s,k}$, ns) of the *N*-glycan glycosidic linkages, as calculated from average values of MD runs A, B, and C for (a) the glycoprotein and (b) the glycopeptide. The values between brackets are standard deviations of $\tau_{eff,k}$'s (see the Appendix) and 90% confidence intervals of $\tau_{s,k}$'s. The 90% confidence intervals are calculated by the combination of upper and lower $\tau_{eff,k}$ values by using the standard deviation interval of the monosaccharide residues involved. Due to a lack of NOE data involving GlcNAc-**2** H-1 of the glycoprotein, neither the $\tau_{eff,k}$ value of GlcNAc-**2** nor $\tau_{s,k}$ values of the Man-**3**-β1−4GlcNAc-**2** and GlcNAc-**2**-β1−4GlcNAc-**1** linkages could be calculated. Therefore, these linkages have been treated as being equally (im)mobile, which is, approximately, probably the case. For comparison the glycopeptide has also been treated this way.

glycopeptide and the glycoprotein are listed in Table 5a (intraresidual ^{1}H−^{1}H pairs) and 5b (interresidual ^{1}H−^{1}H pairs). Obviously, the use of a rotation correlation time for each intraresidual NOE (method III) results in a better overall fit for the intraresidual R_w value than the use of one mean rotation correlation time (method I). This holds for both the glycopeptide and the glycoprotein. The large improvement with method III already points to the importance of taking into account local mobilities within the oligosaccharide chain. The fit of the interresidual NOE intensities with the experimental data indicates the validity of the respective models. Method III also results in smaller interresidual R_w values than method I (Table 5b). The improvement with method III is even better for the glycoprotein than for the glycopeptide. Thus, as already shown for the glycopeptide (Lommerse et al., 1995), it is necessary to take local mobilities into account when calculating NOE intensities for the *N*-glycan as part of the glycoprotein. The R_w values for each individual interresidual NOE of both the glycopeptide and the glycoprotein, as calculated by method III, are listed in Table 6.

Analysis of Mobilities within the Oligosaccharide Chain. The $\tau_{eff,k}$ values and derived slow internal rotation correlation times $\tau_{s,k}$, with standard deviations, for both glycoprotein and glycopeptide are shown in Figure 5. Obviously, the $\tau_{eff,k}$ value of each monosaccharide residue as part of the intact glycoprotein is longer than that as part of the glycopeptide. GlcNAc-**1** is the least mobile monosaccharide residue both in the glycopeptide and in the glycoprotein. In the glycopeptide, GlcNAc-**1** is near the center of mass and mainly experiences the overall motion of the molecule. In the glycoprotein, GlcNAc-**1** is linked to the relatively immobile polypeptide chain. In both the glycopeptide and the glycoprotein, the effective rotation correlation times are shorter when going to more peripheral residues in the oligosaccharide chain, due to the addition of reorientational motions of the glycosidic linkages.

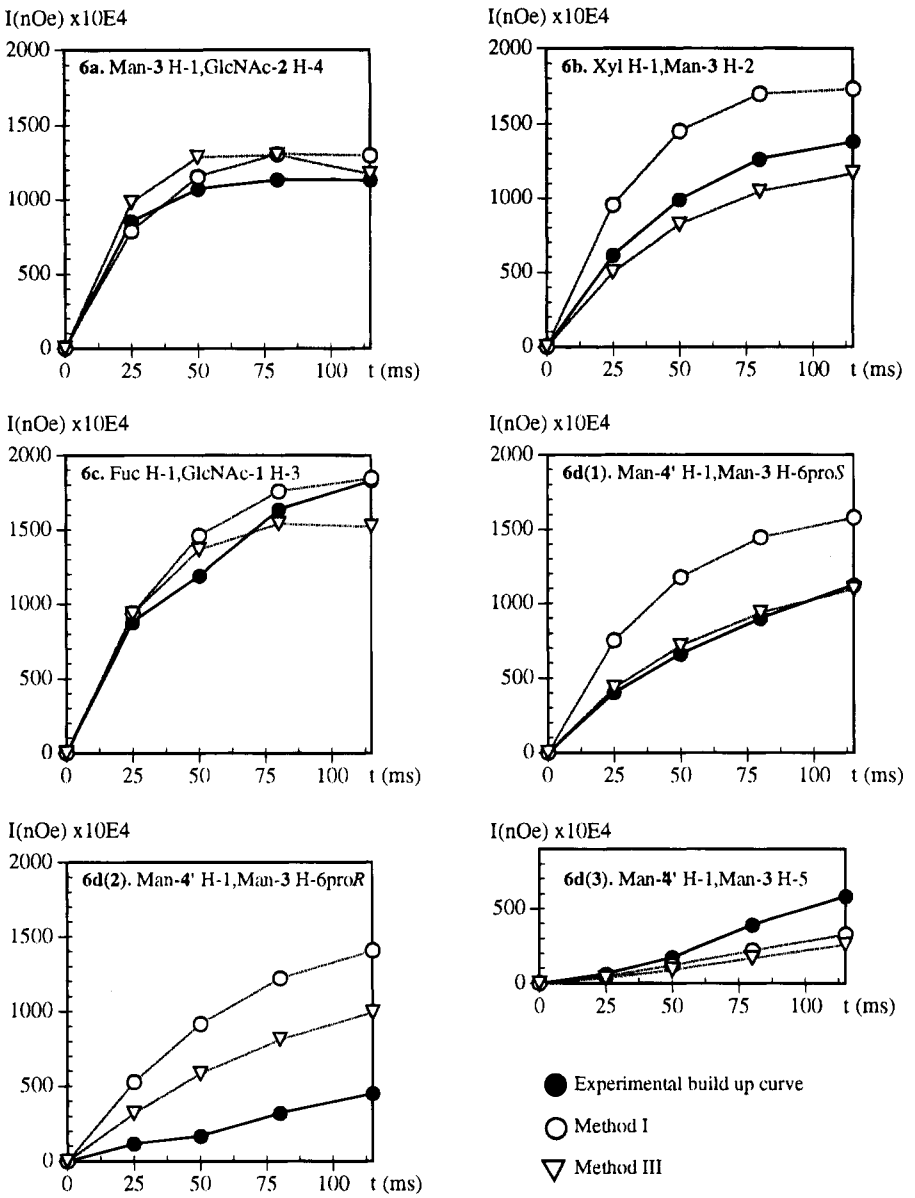

FIGURE 6: NOE build-up curves of interresidual $^1H-^1H$ pairs within the *N*-glycan of intact bromelain (both experimental and calculated using the CROSREL program).

Besides the longer effective rotation correlation times, important differences in the mobility of the glycosidic linkages appear between glycopeptide and glycoprotein, as inferred from the slow internal rotation correlation times ($\tau_{s,k}$, Figure 5). The $\tau_{s,k}$ values reflect the transition rate between minimum energy regions in the ϕ,ψ space of the glycosidic linkage (Lommerse et al., 1995). The linkages within the Xylβ1−2Man-**3**-β1−4GlcNAc-**2**-β1−4GlcNAc-**1** element seem to be rather rigid in both molecules. Large differences between the $\tau_{s,k}$ values appear at the linkages Man-**4'**-α1−6Man-**3** and Fucα1−3GlcNAc-**1**. These linkages are clearly less mobile in the glycoprotein than in the glycopeptide (*vide infra*).

Glycosidic Linkages. In order to study the possible influence of the polypeptide chain on the *N*-glycan conformation, each glycosidic linkage in the oligosaccharide chain of the intact bromelain was compared with the same linkage in the glycopeptide. In Figure 6a−d, the experimental and theoretical interresidual NOE build-up curves of the glycoprotein *N*-glycan are plotted, on the basis of the average oligosaccharide chain model of MD run B. The same model was also used for the glycopeptide (Lommerse et al., 1995).

The theoretical MD models of the linkage *Man-3-β1−4GlcNAc-2* point to one conformational region at ϕ,ψ = −70,125. This conformation is possibly stabilized by the hydrogen bond between GlcNAc-**2** O3 and Man-**3** O5 (34% of the total simulated time). The calculated Man-**3** H-1/GlcNAc-**2** H-4 NOE intensities of the glycoprotein *N*-glycan fit the experimental data very well (Figure 6a). The simulated conformation is expected to be predominant, as has also been concluded for the glycopeptide.

The glycosidic linkage *Xylβ1−2Man-3* is present in one region at ϕ,ψ = −80,−100 during the MD simulations. Xylose is the most mobile residue in the oligosaccharide chain of the glycoprotein, having an effective rotation correlation time about half as long as the mean rotation correlation time of the *N*-glycan. Therefore, it is important to account for this mobility when calculating NOE intensities from the models. The slow internal rotation correlation time ($\tau_{s,k}$ = 7.0 ns) of this glycosidic linkage is not significantly

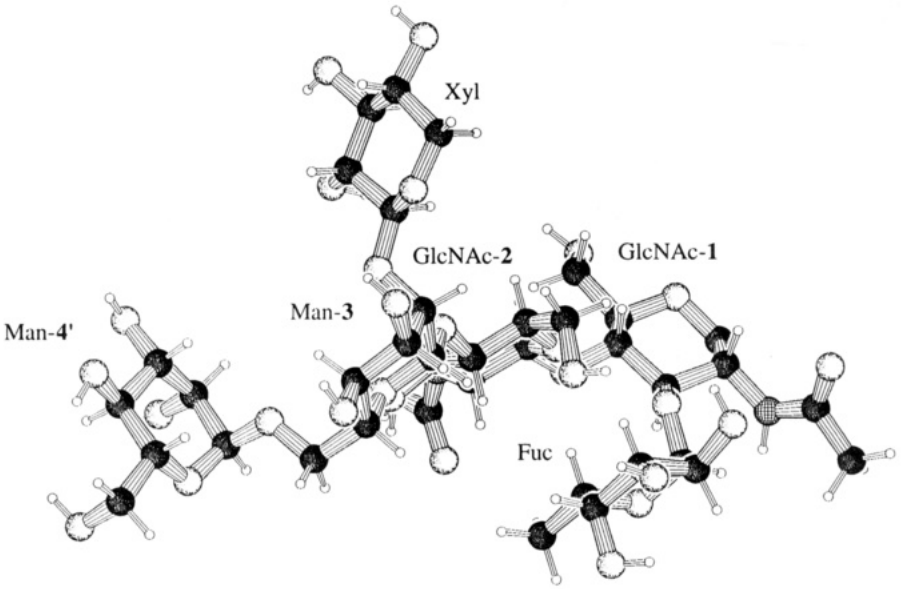

FIGURE 7: Spatial model of the pineapple stem bromelain *N*-glycan.

different from that of the glycopeptide ($\tau_{s,k}$ = 5.8 ns, Figure 5), indicating equal mobility. The calculated Xyl H-1/Man-**3** H-2 NOE intensities of MD trajectory B ($\phi,\psi = -78,-97$) perfectly fit the experimental data, applying method III (Figure 6b). Therefore, the conformation of this glycosidic linkage in the glycoprotein is in the same minimum energy region as was concluded for this linkage in the glycopeptide.

The linkage *Fucα1−3GlcNAc-**1*** showed roughly two stable conformations during the MD simulations of the glycopeptide at $\phi,\psi = -140,-135$ and at $\phi,\psi = -90,-100$, respectively. Several differences appear when comparing the glycoprotein and glycopeptide *N*-glycan data for this linkage. First, the longer slow internal rotation correlation time ($\tau_{s,k}$ = 25 ns *versus* $\tau_{s,k}$ = 2 ns) clearly reveals a lower degree of mobility of the Fucα1−3GlcNAc-**1** linkage in the glycoprotein. Second, the interresidual Fuc H-1/GlcNAc-**1** H-3 NOE intensities point to a different distribution between the simulated minima. Both MD trajectories A (mainly $\phi,\psi = -90,-100$) and B (mainly $\phi,\psi = -140,-135$) reasonably fit the experimental data for the glycoprotein (for run B, see Figure 6c). In contrast, in the glycopeptide only run B gives acceptable agreement. The fits of runs A and C have much improved in the glycoprotein. This indicates that $\phi,\psi = -90,-100$ is more abundant than in the glycopeptide.

The decreased mobility of Fuc is caused by increased energy barriers between low-energy regions in the ϕ,ψ surface, possibly due to specific interactions between the polypeptide chain and Fuc or between the polypeptide chain and GlcNAc-**1** N-H. In the latter case, GlcNAc-**1** N-H might not be available to lower the energy barrier between the $\phi,\psi = -140,-135$ and $\phi,\psi = -90,-100$ conformations by hydrogen bond formation between GlcNAc-**1** N-H and Fuc O2, as was the case in the glycopeptide (Lommerse et al., 1995). Hydrogen bond formation between the Fuc and GlcNAc-**1** residues and the amino acid residues has also been found from X-ray studies on a lectin of *Erythrina corallodendron* (Ecorl; Shaanan et al., 1991). The Ecorl glycoprotein contains the *N*-glycan of pineapple stem bromelain, extended by an extra mannose residue, forming a Man-**4**-α1−3Man-**3** linkage.

The Man-**4′** residue is usually considered a very mobile residue because of the extra dihedral angle ω at the glycosidic linkage *Man-**4′**-α1*−6Man-**3**. The rotamer distribution of the oxymethyl group of Man-**3** could not be determined for the intact glycoprotein *N*-glycan, because it was not possible to determine the vicinal coupling constant $^3J_{H5-H6pro\text{-}R}$. It should be noted that it was possible to calculate this rotamer distribution in the denatured glycoprotein by using $^3J_{H5-H6pro\text{-}R}$ (3.6 ± 0.8 Hz) and $^3J_{H5-H6pro\text{-}S}$ (1.5 ± 0.8 Hz) measured on the Man-**3** H-2 track in the HOHAHA spectrum (Figure 4). By applying the empirical generalized Karplus equation (Haasnoot et al., 1980), a predominantly *gg* conformation (~80%) for Man-**3** was determined, which is slightly different from that of the glycopeptide (>98%; Bouwstra et al., 1990).

Evidence for the presence of the Man-**3** *gt* conformation in the intact glycoprotein *N*-glycan was found by the interresidual Man-**4′** H-1/Man-**3** H-5 NOE intensities. The S shape of the experimental NOE build-up curve (Figure 6d(3)) indicates some spin diffusion. However, only 50% of the Man-**4′** H-1/Man-**3** H-5 NOE intensities can be attributed to spin diffusion via Man-**3** H-6-*pro-S*, as calculated for all theoretical models studied here (Table 3). The other 50% of these NOE intensities have to be explained by a direct NOE transfer between the protons involved. This is only possible if the Man-**3** *gt* rotamer occurs for a significant period of time, in conjunction with the $\phi,\psi = 70,100$ conformation at the Man-**4′**-α1−6Man-**3** linkage (Bouwstra et al., 1989). The $\phi,\psi,\omega = 70,100,60$ conformation has also been observed by X-ray analysis of Ecorl (Shaanan, 1991). As a consequence of very small Man-**4′** H-1/Man-**3** H-6-*pro-R* NOE intensities in the $\phi,\psi,\omega = 70,100,60$ conformation, the contribution of this conformation will also improve the fit because the current MD simulations result in values too large for this NOE (Table 6).

Man-**4′** in the glycoprotein is a mobile residue compared to the other residues in the oligosaccharide chain. However, the slow internal rotation correlation time ($\tau_{s,k}$ = 9.5 ns) indicates that the glycosidic linkage clearly has reduced mobility, as compared with this linkage of the glycopeptide ($\tau_{s,k}$ = 1.5 ns). This holds even at the higher temperature for the NOESY experiment of the glycoprotein, pointing to an interaction of Man-**4′** with the polypeptide chain.

The fit of both Man-**4′** H-1/Man-**3** H-6-*pro-S* and Man-**4′** H-1/Man-**3** H-6-*pro-R* NOE intensities to the experiment are similar for the glycopeptide and for the glycoprotein, implying comparable distributions of ϕ,ψ conformations in these compounds. However, the direct NOE transfer of the interresidual Man-**4′** H-1/Man-**3** H-5 contact, being absent from the glycopeptide (Bouwstra et al., 1990; Lommerse et al., 1995), also points to the presence of the ϕ,ψ = 70,100 conformation for part of the time in the glycoprotein.

CONCLUSIONS

The ^{1}H NMR NOESY measurements of the pineapple stem bromelain *N*-glycan were accompanied by some denaturation at 315 K, resulting in two sets of clearly distinct ^{1}H NMR signals: one set for the *N*-glycan protons as part of the intact glycoprotein and one set for the *N*-glycan protons as part of the denatured form. The intact glycoprotein *N*-glycan experiences a different environment and is less mobile than the *N*-glycan of the denatured glycoprotein, as shown by the differences in proton chemical shifts of the *N*-glycan and by the larger line widths of the carbohydrate signals. This is possibly caused by interaction of the intact glycoprotein *N*-glycan with the polypeptide chain, whereas the relative mobility of the denatured glycoprotein *N*-glycan is probably due to (local) unfolding of the polypeptide chain.

The effective rotation correlation times ($\tau_{\mathrm{eff},k}$'s) of the constituent monosaccharide residues, as well as the slow internal rotation correlation times ($\tau_{\mathrm{s},k}$'s) of the glycosidic linkages, for the *N*-glycan as part of the glycoprotein and as part of the glycopeptide are summarized in Figure 5. In both cases, the GlcNAc-**1** residue experiences the longest $\tau_{\mathrm{eff},k}$, due to its attachment to the polypeptide chain in the glycoprotein and its position near the center of mass in the glycopeptide. The $\tau_{\mathrm{eff},k}$'s are shorter when going to more peripheral residues, showing a larger degree of mobility of these residues in both *N*-glycans. The mean rotation correlation time of the *N*-glycan as part of the intact glycoprotein (τ_o = ±9 ns) is much larger than that of the glycopeptide (τ_o = ±0.7 ns), as a consequence of its attachment to the large polypeptide chain. The internal rotation correlation times point to the relative rigidity of the Xylβ1−2Man-**3**-β1−4GlcNAc-**2**-β1−4GlcNAc-**1** element in both the glycoprotein and the glycopeptide *N*-glycans, but the Fucα1−3GlcNAc-**1** and Man-**4′**-α1−6Man-**3** linkages clearly are more mobile in the glycopeptide than in the glycoprotein.

The Fucα1−3GlcNAc-**1** linkage in the intact glycoprotein has a different distribution between the two minima at ϕ,ψ = −90,−100 and ϕ,ψ = −140,−135, of which the latter seems to be more abundant in the glycopeptide. This glycosidic linkage clearly is less mobile in the intact glycoprotein. These findings might be a direct effect of the close proximity of Fuc to the polypeptide chain, giving rise to steric hindrance and/or hydrogen bond formation between the *N*-glycan and the polypeptide chain.

In contrast to the glycopeptide *N*-glycan, the Man-**3** *gt* (ω = 60) rotamer is probably present in the intact glycoprotein *N*-glycan. The mobility of the Man-**4′**-α1−6Man-**3** linkage is reduced in comparison with this linkage in the glycopeptide. This can be the result of an interaction of the polypeptide chain with the Man-**4′**/Fucα side of the oligosaccharide chain (Figure 7). The unaffected mobility of the Xyl residue shows that Xyl is situated in the bulk solution. An interaction between a mannose residue and the polypeptide chain has also been suggested for the high mannose glycan of human T lymphocyte glycoprotein CD2 (Withka et al., 1993). In CD2, a mannose residue on the fourth or fifth position in the carbohydrate chain would form hydrogen bonds with the polypeptide chain.

In summary, this detailed conformational study shows that caution must be taken when transferring the conformational data of an oligosaccharide or a glycopeptide to the glycan as part of a glycoprotein. By using alternative NMR techniques, such as heteronuclear ^{1}H−^{13}C experiments, more information can be gained about the solution conformation of glycoprotein glycans in their natural environments: specifically, if one can identify possible NOE interactions between the skeleton carbohydrate protons and those of the polypeptide chain. Futher studies are in progress to obtain a better understanding of the conformational behavior of the pineapple stem bromelain *N*-glycan.

ACKNOWLEDGMENT

We thank Dr. H. H. J. de Jongh for his help in recording CD spectra.

APPENDIX

The CROSREL program (Leeflang & Kroon-Batenburg, 1992) applies a full relaxation rate matrix analysis by using the generalized Bloch equations. The time dependency of the (cross) peak intensities in a 2D NOESY spectrum is given by

$$\mathbf{A}(\tau_m) \approx \mathbf{M}_0\, e^{(-\mathbf{R}\tau_m)} \approx 1 - \mathbf{R}\tau_m + {}^1/_2\mathbf{R}^2\tau_{m-\ldots}^2 \quad \text{(A1)}$$

wherein τ_m is the mixing time for magnetization transfer, $\mathbf{M}_0$ is the initial magnetization of a nucleus at $\tau_m = 0$, **A** is the NOE matrix, and **R** is the relaxation rate matrix.

The NOE intensity of the proton pair i,j, given that the cross relaxation rates $\sigma_{ij} = \sigma_{ji}$, is then approximated by

$$a_{ij}(\tau_m) = -\sigma_{ij}\tau_m + {}^1/_2[(\varrho_{ii} + \varrho_{jj})\sigma_{ij} + \sum_{k\neq i,k\neq j,k=1}^{n} \sigma_{ik}\sigma_{jk}]\tau_m^2 \quad \text{(A2)}$$

with ϱ_{ii} representing the diagonal elements of **R**. This leads to a parabolic shape of an NOE build-up curve:

$$a_{ij}(\tau_m) = c_1\tau_m + c_2\tau_m^2 \quad \text{(A3)}$$

For large macromolecules the cross relaxation rate is linear with $\tau_{\mathrm{eff},k}$:

$$\sigma_{ij} = -C\langle r_{ij}^{-3}\rangle^2\tau_{\mathrm{eff},k} \quad \text{(A4)}$$

thus, c_1 is proportional to τ_{eff}. Therefore, the relative standard deviation obtained for c_1 from a fit of an NOE build-up curve to eq A3 is equal to that of τ_{eff}.

REFERENCES

Baker, E. N. (1980) *J. Mol. Biol. 141*, 441−484.

Bax, A., & Davis, D. G. (1985) *J. Magn. Reson. 65*, 355−360.
Bouwstra, J. B., Leeflang, B. R., D'Andrea, G., Oerlemans, M., Kamerling, J. P., & Vliegenthart, J. F. G. (1989) Thesis, Utrecht University, Utrecht, The Netherlands, Chapter 5.
Bouwstra, J. B., Spoelstra, E. C., De Waard, P., Leeflang, B. R., Kamerling, J. P., & Vliegenthart, J. F. G. (1990) *Eur. J. Biochem. 190*, 113−122.
Brockbank, R. L., & Vogel, H. J. (1990) *Biochemistry 29*, 5574−5583.
Chang, C. T., Wu, C.-S. C., & Yang, J. T. (1978) *Anal. Biochem. 91*, 13−31.
Greenfield, N., & Fasman, G. D. (1969) *Biochemistry 8*, 4108−4116.
Haasnoot, C. A. G., De Leeuw, F. A. A. M., & Altona, C. (1980) *Tetrahedron 36*, 2783−2792.
Ishihara, H., Takahashi, N., Oguri, S., & Tejima, S. (1979) *J. Biol. Chem. 254*, 10715−10719.
IUPAC−IUB Joint Commission on Biochemical Nomenclature (JCBN) (1983) *Eur. J. Biochem. 131*, 5−7.
Joziasse, D. H., Schiphorst, W. E. C. M., Van den Eijnden, D. H., Van Kuik, J. A., Van Halbeek, H., & Vliegenthart, J. F. G. (1987) *J. Biol. Chem. 262*, 2025−2033.
Kamphuis, I. G., Kalk, K. H., Swarte, M. B. A., & Drenth, J. (1984) *J. Mol. Biol. 179*, 233−256.
Kamphuis, I. G., Drenth, J., & Baker, E. N. (1985) *J. Mol. Biol. 182*, 317−329.
Leeflang, B. R., & Kroon-Batenburg, L. M. J. (1992) *J. Biol. NMR 2*, 495−518.
Lommerse, J. P. M., Kroon-Batenburg, L. M. J., Kroon, J., Kamerling, J. P., & Vliegenthart, J. F. G. (1995) *J. Biol. NMR* (in press).
Macura, S., & Ernst, R. R. (1983) *J. Magn. Reson. 53*, 521−528.
Press, W. H., Flannery, B. P., Teukolsky, S. A., & Vetterling, W. T. (1986) in *Numerical Recipes*, pp 509−515, Cambridge University Press, Cambridge, UK.
Ritonja, A., Rowan, A. D., Buttle, D. J., Rawlings, N. D., Turk, V., & Barrett, A. J. (1989) *FEBS Lett. 247*, 419−424.
Rowan, A. D., Buttle, D. J., & Barrett, A. J. (1988) *Arch. Biochem. Biophys. 267*, 262−270.
Shaanan, B., Lis, H., & Sharon, N. (1991) *Science 254*, 862−866.
Topham, C. M., Overington, J., Kowlessur, D., Thomas, M., Thomas, E. W., & Brocklehurst, K. (1990) *Biochem. Soc. Trans. 18*, 579−580.
Van Kuik, J. A., Hoffmann, R. A., Mutsaers, J. H. G. M., Van Halbeek, H., Kamerling, J. P., & Vliegenthart, J. F. G. (1986) *Glycoconjugate J. 3*, 27−34.
Vargese, J. N., & Colman, P. M. (1991) *J. Mol. Biol. 221*, 473−486.
Vliegenthart, J. F. G., Dorland, L., & Van Halbeek, H. (1983) *Adv. Carbohydr. Chem. Biochem. 41*, 209−374.
Withka, J. M., Wyss, D. F., Wagner, G., Arulanandam, A. R. N., Reinherz, E. L., & Recny, M. A. (1993) *Structure 1*, 69−81.
Wüthrich, K. (1986) *NMR of proteins and nucleic acids*, John Wiley & Sons, New York.
Yang, J. T., Wu, C.-S. C., & Martinez, H. M. (1986) *Methods Enzymol. 130*, 208−269.

BI942865T